J. Fluid Mech. (1999), *vol.* 391, *pp.* 29–44. Printed in the United Kingdom

© 1999 Cambridge University Press

Evolution of vortex knots

By RENZO L. RICCA[1]†, DAVID C. SAMUELS[2] AND CARLO F. BARENGHI[2]

[1]Department of Mathematics, University College London, Gower Street, London WC1E 6BT, UK
e-mail: ricca@math.ucl.ac.uk
[2]Department of Mathematics, University of Newcastle, Newcastle upon Tyne, NE1 7RU, UK

(Received 24 November 1997 and in revised form 18 January 1999)

For the first time since Lord Kelvin's original conjectures of 1875 we address and study the time evolution of vortex knots in the context of the Euler equations. The vortex knot is given by a thin vortex filament in the shape of a torus knot $\mathscr{T}_{p,q}$ ($p > 1$, $q > 1$; p, q co-prime integers). The time evolution is studied numerically by using the Biot–Savart (BS) induction law and the localized induction approximation (LIA) equation. Results obtained using the two methods are compared to each other and to the analytic stability analysis of Ricca (1993, 1995). The most interesting finding is that thin vortex knots which are unstable under the LIA have a greatly extended lifetime when the BS law is used. These results provide useful information for modelling complex structures by using elementary vortex knots.

1. Introduction

Lord Kelvin was the first (see Kelvin 1875, p. 123, ¶16) to speculate on the existence of vortex knots in ideal fluids and to conjecture that thin vortices in the shape of torus knots were stable under the Euler equations. From a mathematical viewpoint the question was left open, and it still represents a stimulating challenge to mathematicians. In this paper we address Lord Kelvin's conjecture by studying vortex knot evolution under both the Biot–Savart (BS) law and the localized induction approximation (LIA) equation, testing the stability results based on LIA analysis and determining the long-term evolution of torus knots by direct numerical integration of the governing equations.

Applications of ideas from modern topology to fluid mechanics have been pioneered by Moffatt and co-workers (Moffatt 1969; Berger & Field 1984; Moffatt & Tsinober 1990; Moffatt *et al.* 1992; Moffatt & Ricca 1992; Ricca & Berger 1996; Ricca 1998), whose results clearly demonstrate the importance of the new techniques in the study of knotted and linked structures in fluid flows. The existence of topologically complex solutions to dynamical systems is well documented in the literature (see, for example, Birman & Williams 1983; Holmes & Williams 1985), and the use of geometric and topological methods in fluid mechanics has indeed proven to be very useful in the analysis of the entanglement of filamentary vortex structures as observed in direct numerical simulations of turbulent flows (see, for example, Kerr 1985; She, Jackson & Orszag 1990; Vincent & Meneguzzi 1991; Jiménez *et al.* 1993). The most advanced visiometrics (Zabusky, Silver & Pelz 1993; Fernandez, Zabusky & Gryanik

† Author to whom correspondence should be addressed.

https://doi.org/10.1017/S0022112099005224 Published online by Cambridge University Press

1995) of streamlines and vorticity lines associated with the formation of coherent structures reveal that a high degree of braiding, re-connection and formation of new linkings of fluid structures is a generic feature of turbulent flows. The study of complex flow patterns using topological techniques finds useful applications in the study of filamentary structures present on a wide spectrum of physical scales, from solar coronal loops in magneto-hydrodynamics (Bray *et al.* 1991; Berger 1993) and tornadoes in geophysical fluid dynamics (Lugt 1983), to quantized vortex lines in superfluidity (Donnelly 1991; Barenghi 1997) and superconductivity (Berger & Rubinstein 1997). Yet, from a theoretical viewpoint very little is known of the long-term evolution of topologically complex structures and of the influence of global geometry and topology on the dynamics. There is therefore a call for more information about these processes and their mathematical modelling.

Coherent structures, such as the thick vortex tubes present in classical fluids or the thin vortex filaments in superfluid helium, can be thought of as made up of a bundle of elementary vortex lines aligned along the tube axis. If the geometry of vortex lines is responsible for the dynamics of a vortex tangle, topological properties represent an important ingredient in the mathematical description of the flow field. Relationships between geometric and topological properties are very subtle and very little explored. Simple geometries of vortex flows (such as vortex rings) may have complex topology in terms of the constituent vortex lines, while apparently complex tangles of vortex lines may correspond to a trivial topology (an example of which is given by the simple twist of a pair of trailing vortices). In a sense topological complexity can be regarded as an additional feature of the flow field. A vortex ring with vortex lines twisted about the torus centreline provides a good example of non-trivial topology of the constituent flow field. The twisting of the vortex lines gives the structure topological linking and contributes to the kinetic helicity of the vortex ring (Moffatt & Ricca 1992).

In mathematical terms topological complexity of field lines is realized through knots and links. In the vortex ring case complex topology of vortex lines can be achieved in two fundamental ways. One is through high twisting and linking of vortex lines; the other is through knotting. Torus knots are good candidates to model complex structures. Their geometry can be easily described in terms of closed curves wound around a mathematical torus (for a proper definition of torus knots see § 2), while topology can be prescribed to achieve a high degree of complexity (useful to model, for example, turbulent vortex tangles). Torus knots are also closely related to a class of 'unknots' (i.e. unknotted closed curves given by a multiple folding of the standard circle; see § 2 below), that provide interesting new test cases for studying the evolution of vortex geometries. In this paper we shall study the time evolution of thin vortex filaments in the shape of torus knots and related 'unknots'.

A coherent bundle of vortex lines, either knotted or linked together, has a decidedly non-trivial topology. In the context of the Euler equations, vortex structures move while conserving the topology of the system. This is a fundamental property of inviscid evolution and is encapsulated in the formal integrals of the Cauchy equations. In the absence of viscosity vortex lines are free to move in the fluid, preserving the knot and link types that tie them together. Since topology is 'frozen' in the fluid, vortex evolution is influenced by the topology of the system.

In real fluids, though, the presence of viscosity and dissipative effects allows reconnections of vortex lines to take place, and in the presence of reconnections topology is bound to change. However, as long as vortex elements are not too close to one another, Euler's equations still provide a good approximation to real vortex dynamics.

https://doi.org/10.1017/S0022112099005224 Published online by Cambridge University Press

In many practical situations, where vorticity is highly localized, coherence of vortex structures survives for a considerable time. In these cases vortex filaments can be considered as ideal entities, governed by an evolution that is still little influenced by viscous effects. As vortex elements come into contact, dissipative effects become dominant over coherence and can no longer be neglected. Under reconnection we have a sudden, dramatic change in the geometry and topology of the flow pattern. An accurate model of the reconnection mechanism must take into account detailed information about the physics of the fluid and the viscous processes involved. We have a similar situation when we consider the interaction of fluid structures in electrically charged plasmas, which are important for geophysical and astrophysical applications. In this case dissipative effects are given not only by viscous forces, but also by resistive effects present in the fluid medium (Bray *et al.* 1991). Vortex interaction in superfluids is also an important phenomenon. Here superfluid vortex lines interact according to the laws of quantum mechanics (Koplick & Levine 1993). In this case the inviscid model is still a very good approximation at a macroscopic level, that is as long as the typical interaction scale length is greater than the quantum mechanical healing length (of the order of 10^{-10} m).

In ideal conditions vortex motion is governed by the Biot–Savart law (BS) (see Batchelor 1967; Saffman 1992), which is a global functional of vorticity. Consider an isolated vortex line $\mathscr{C}$ of strength Γ, embedded in a domain $\mathscr{D} \subseteq \mathbb{R}^3$ entirely filled by an ideal, incompressible fluid. The vortex line moves with a self-induced velocity $\boldsymbol{u}(\boldsymbol{X})$ ($\boldsymbol{X}$ is the position vector in $\mathbb{R}^3$), given by

$$\boldsymbol{u}(\boldsymbol{X}) = \frac{\Gamma}{4\pi} \int_{\mathscr{C}} \frac{\hat{\boldsymbol{t}} \times (\boldsymbol{X} - \boldsymbol{R}(s))}{|\boldsymbol{X} - \boldsymbol{R}(s)|^3} \mathrm{d}s, \tag{1}$$

where $\boldsymbol{X} = \boldsymbol{R}(s)$ is the vector equation for $\mathscr{C}$, s is arclength and $\hat{\boldsymbol{t}} \equiv \mathrm{d}\boldsymbol{R}/\mathrm{d}s$ the unit tangent along $\mathscr{C}$. Equation (1), which governs the Euler evolution, retains all the induction effects associated with the whole geometry of $\mathscr{C}$ and preserves vortex topology. Explicit analytic solutions to the BS law are difficult to obtain and until now only circular and helical geometries have been studied in detail. Moreover, numerical simulations based on (1) are rather expensive to run because the motion of each single vortex point depends on the motion of all the other constituent points into which the vortex line is discretized. To overcome these difficulties several asymptotic techniques have been proposed, and work in this direction is still in progress (see, for example, the comparative study carried out by Zhou 1997 on the implementation of various asymptotic techniques).

The crudest approximation to the BS law was derived by Da Rios almost a century ago (see the review article by Ricca 1996), and is based on the so-called localized induction approximation (LIA). By neglecting non-local (long-range) effects and self-interactions of different parts of the vortex, LIA gives a first-order approximation to the motion of the vortex filament. Under LIA the motion is essentially governed by local curvature effects and in the limit of very thin vortex filaments this is given by

$$\boldsymbol{u}_{\mathrm{LIA}} = \frac{\Gamma}{4\pi} \ln \delta \boldsymbol{R}' \times \boldsymbol{R}'' = \frac{\Gamma c}{4\pi} \ln \delta \hat{\boldsymbol{b}}, \tag{2}$$

where c and $\hat{\boldsymbol{b}}$ are the curvature and unit binormal vector of $\mathscr{C}$, and δ is a measure of the aspect ratio of the vortex. Here we consider only thin vortex filaments, hence we take $\delta = \text{const.} \gg 1$. Because of the approximations involved, the LIA is of limited applicability in classical vortex dynamics. However, we should remember that also in

https://doi.org/10.1017/S0022112099005224 Published online by Cambridge University Press

the numerical implementation of the BS law we still have the problem of a logarithmic singularity, present in the integrand of equation (1) when $\boldsymbol{X}$ approaches $\boldsymbol{R}$. In this case the standard procedure, which we shall follow (see § 3 below), and that is used extensively in the literature (see, for example, Leonard 1980, 1985; Moin, Leonard & Kim 1986; Leonard & Chua 1989; Fernandez *et al.* 1995), is to de-singularize the BS integral by using a cut-off length l, substituting the singular BS part with the corresponding LIA dynamics. In a sense, the cut-off length plays the role of a smoothing mechanism for the physics of the singularity, where viscous, resistive or quantum effects are dominant. We should remember, however, that there are physical contexts in which the LIA represents a good approximation. The LIA indeed finds useful application in studies of filament dynamics for defect formation in micro-physics (Lugomer 1998), and in modelling helium superfluid turbulence, where long-range effects tend to cancel each other out (see the discussion in Barenghi *et al.* 1998). Moreover, the mathematical simplicity of the LIA offers considerable analytical and numerical advantages to exploit, one of these being the study of knotted vortex structures.

2. Torus knots as steady solutions to the LIA equation

The only analytical results on vortex knots are based on the LIA equation applied to thin vortex filaments in the shape of torus knots. In their standard representation torus knots are particularly symmetric knots embedded in a mathematical torus Π. Let us recall a fundamental theorem of Massey (1967):

THEOREM 1. *A closed, non-self-intersecting curve embedded in* Π, *that cuts a meridian at* $p > 1$ *points and a longitude at* $q > 1$ *points* (p *and* q *relatively prime integers*), *is a non-trivial knot* $\mathscr{T}_{p,q}$, *with winding number* $w = q/p$.

The *winding number* w is a topological invariant of the knot type and is a measure of the average number of wraps of the knot along the small circle of the torus Π (in the meridian plane), per number of wraps along the torus circular axis (in the longitudinal plane). For given p and q, the two knots obtained by exchanging p and q are topologically equivalent, i.e. $\mathscr{T}_{p,q} \sim \mathscr{T}_{q,p}$. This means that for fixed p and q, $\mathscr{T}_{p,q}$ and $\mathscr{T}_{q,p}$ represent the *same* knot and can be deformed one into the other by continuous deformations (i.e. without cuts; see the two examples of figure 1*a*). However, when $p = 1$ and/or $q = 1$, the closed curve is not knotted (the curve is called the 'unknot'), since it can be isotoped by continuous deformations to the standard circle (the standard unknot $\mathscr{U}_\circ$). From a geometric viewpoint the unknots associated with the family of torus knots are interesting curves. We can group them into two distinct families: 'toroidal' coils (denoted by $\mathscr{U}_{m,1}$ in figure 1*b*), and 'poloidal' coils (denoted by $\mathscr{U}_{1,m}$). For given m, $\mathscr{U}_{m,1}$ is equivalent to a closed curve wrapped around Π m times in the longitudinal direction and only once in the meridian direction, whereas $\mathscr{U}_{1,m}$ is a closed curve wrapped around Π m times in the meridian direction and only once in the longitudinal direction. Evidently, these unknots are all topologically equivalent to the standard circle, i.e. $\mathscr{U}_{m,1} \sim \mathscr{U}_{1,m} \sim \mathscr{U}_\circ$.

Vortex knots, unlike their mathematical counterpart, are dynamical objects that evolve under the laws of vortex motion, prescribed by the Euler equations, which govern the motion of the physical knot. Here an interesting question is whether a given vortex torus knot type can evolve freely to its own corresponding isotope. Since vortex dynamics is determined primarily by geometric aspects, different geometries of the same vortex knot type may lead to different configurations. In the case of LIA, the dynamics can be re-written by appropriate re-scaling of time in the simplified

https://doi.org/10.1017/S0022112099005224 Published online by Cambridge University Press

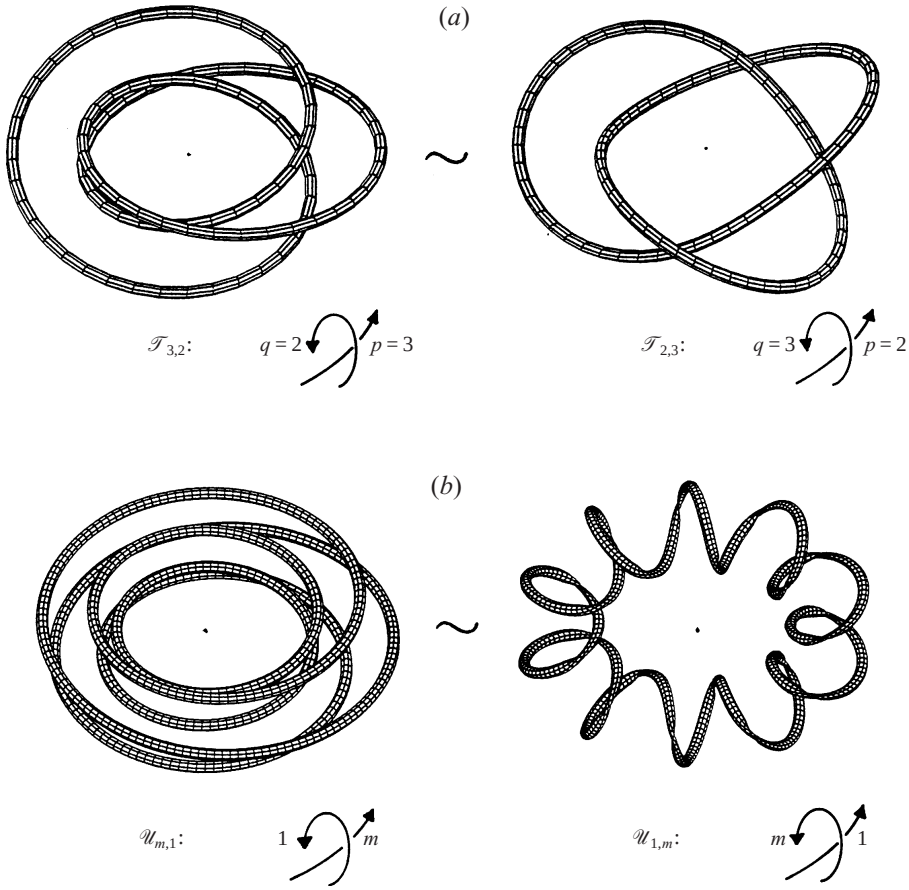


FIGURE 1. (*a*) Two different geometries of the trefoil knot. In terms of the topological classification of knot types this represents the first member of the family of torus knots $\mathscr{T}_{p,q}$: the standard form is given by the $\mathscr{T}_{2,3}$ knot on the right, which can be isotoped by continuous deformations to the $\mathscr{T}_{3,2}$ knot on the left. These two knots are topologically equivalent, hence they represent the same knot type. (*b*) The standard circle (the 'unknot' $\mathscr{U}_\circ$) can take the shape of a toroidal coil $\mathscr{U}_{m,1}$, or a poloidal coil $\mathscr{U}_{1,m}$. In pure topological terms, though, all the unknots are equivalent to trivial objects.

form

$$\boldsymbol{u}_{\mathrm{LIA}} = c\hat{\boldsymbol{b}}. \tag{3}$$

We have the following theorem (Kida 1981):

THEOREM 2. *Let $\mathscr{K}_v$ denote the embedding of a knotted vortex filament in an ideal fluid in $\mathscr{D}$. If $\mathscr{K}_v$ evolves under LIA, then there exists a class of steady solutions in the shape of torus knots $\mathscr{K}_v \equiv \mathscr{T}_{p,q}$.*

Kida finds solutions in terms of fully nonlinear relationships that involve elliptic functions of travelling waves. A more direct and simple approach (Ricca 1993), based on linear perturbation techniques and cylindrical polar coordinates (r, α, z), gives 'small-amplitude' torus knot solutions (asymptotically equivalent to the Kida solutions), that are more easily handled analytically and numerically. These solutions

https://doi.org/10.1017/S0022112099005224 Published online by Cambridge University Press

are given by

$$\left.\begin{aligned} r &= r_0 + \epsilon_0 k_r \sin(w\phi + \phi_0), \\ \alpha &= \frac{s}{r_0} + \epsilon_0 \frac{k_r}{w r_0} \cos(w\phi + \phi_0), \\ z &= \frac{\hat{t}}{r_0} + \epsilon_0 k_r \left(1 - \frac{1}{w^2}\right)^{1/2} \cos(w\phi + \phi_0), \end{aligned}\right\} \tag{4}$$

where r_0 is the radius of the torus circular axis and $\epsilon_0 = a/r_0 \ll 1$ is the inverse of the aspect ratio of the vortex, with a the radius of the vortex cross-section and $k_r = O(r_0)$ a scale factor. Moreover $\phi = (s - kt)/r_0$, with t time, k the wave speed; $\hat{t}$ is time re-scaled with the vortex circulation and ϕ_0 a constant.

An immediate consequence of (4) is the following linear stability result (Ricca 1995):

THEOREM 3. *Let $\mathcal{T}_{p,q}$ denote the embedding of a 'small-amplitude' vortex torus knot $\mathcal{K}_v$ evolving under LIA. $\mathcal{T}_{p,q}$ is steady and stable under linear perturbations iff $q > p (w > 1)$.*

This represents the only known, rigorous result on stability of vortex knots and gives us the motivation to test and carry out numerical experiments on the dynamics of these knots. Remember that equations (4) are not the exact, fully nonlinear solutions to the BS law, but they represent small-amplitude knot solutions to LIA. Anyway, since (4) represent torus knots in physical space, we can also use these equations to investigate vortex knot behaviour under the full BS law, using a code that takes into account global induction effects. Hence, we take equations (4) and (by replacing $(1 - 1/w^2)$ with $|1 - 1/w^2|$ to also allow the study of knots with $w < 1$) we run the appropriate code not only under the LIA equation (so that we can check the result of Theorem 3), but also under the full self-induction law given by the BS integral. Evidently, a numerical investigation of the time evolution of vortex knots (using BS or LIA) is not equivalent to studying the stability of these structures: here we do not take a basic solution and study its perturbation to determine whether infinitesimal disturbances decrease or grow exponentially with time. Rather, we integrate in time the (approximate) knot solutions to the LIA, by letting them evolve under non-local (BS) and local (LIA) self-induction effects. One obvious drawback associated with the use of numerical codes is the (unavoidable) presence of numerical noise, which clearly limits the integration process.

In spite of these limitations, the numerical study can give us some useful insight into the evolution of topologically more complex structures. We should remember that so far we have no direct, experimental evidence of existence of vortex knots. To make progress beyond Theorems 2 and 3, we need to test these results and check whether vortex knot evolution reveals features that are dynamically significant. In particular, we would like to find out how robust is the evolution of these knotted vortex filaments, to what extent these structures evolve by conserving topological and geometric features of physical interest, and when they unfold and break up. The question then arises of whether these vortex structures evolve by preserving a 'geometric signature' that makes them recognizable in terms of their original configuration. Dynamics that preserve topology and geometric features such as mean curvature, mean torsion, writhing number, asymptotic crossing number, etc., while allowing large-amplitude deformations, have not been studied before and there is a lack of rigorous definition and analysis. Here we would like to propose a new definition of stability in relation

https://doi.org/10.1017/S0022112099005224 Published online by Cambridge University Press

to these kind of evolutions. If we take into account large-amplitude perturbations, for example, we can extend the usual concept of Lyapunov stability to include those dynamics governed by geometric signature-preserving flows. The corresponding motion is characterized by finite, large-amplitude (Lyapunov) stable evolutions that maintain their geometric coherence and signature for some (finite) time of physical interest. Hence, we can talk of vortex structures evolving under 'stable' dynamics according to the following

Definition. A vortex structure is said to be (Lyapunov) *stable* if it evolves under signature-preserving flows that conserve topology, geometric signature and vortex coherency.

Stable structures are therefore those able to travel a considerable distance (much larger than their typical size), while preserving their geometric signature for some finite time. If they unfold and break up in a short time (compared with the typical time scale), we shall call them *unstable*. Our task will be to detect whether there are stable evolutions of vortex knots of physical significance.

3. Numerical study of the evolution of vortex knots

To investigate the evolution of torus knots using the LIA and BS law we use an algorithm that sub-divides the initial vortex configuration into N points. The evolution of the vortex is obtained by integrating the equation of motion in time at each point. The algorithm and the computer code that involve the simultaneous adjustment of the N points and the time-step size (as well as tests of the computer code itself) have been discussed extensively in the literature (Schwarz 1988; Aarts & deWaele 1993). As in the pioneering work of Schwarz (1988), the code has been used to study the dynamics of tangles of vortex lines in superfluid turbulence (Samuels 1992) and other aspects of vortex dynamics in superfluid helium (Barenghi *et al.* 1998; Samuels, Barenghi & Ricca 1998) and in classical turbulence (Samuels 1998). For the present simulations the typical time-step values range from 0.01 to 0.03, but they can take values of the order of 0.001 in the vicinity of self-intersecting vortex lines, with N ranging from 100 to 400, depending on the knot type. In some runs, in which we measure the time $T_{\rm rec}$ elapsed at the occurrence of the first self-intersection (see § 4 below), we find that doubling N from 400 to 800 produces only a 1% change in $T_{\rm rec}$.

The numerical study is carried out for the first few torus knots, such as $\mathscr{T}_{2,3}$ and $\mathscr{T}_{3,4}$ and their isotopes, for ϵ_0 ranging between 0.1 and 0.01. A more extensive investigation of knots with higher crossing number is limited by the larger number of mesh points needed to represent these knots. However, for the knots examined the results show generic features and the same qualitative behaviour. The calculation is non-dimensionalized by choosing the radius of the torus circular axis $r_0 = 1$, which sets the length scale, and the vortex filament strength $\Gamma = 1$, which sets the time scale. This leaves the problem of choosing an effective core size $r_{\rm core}$ for the vortex filament. This core size is specified in the LIA equation (see (2) and (3) above), where its choice is related to the choice of the time scale. The effective core size plays a more subtle role in the BS calculation, where it is used to eliminate the singularity present in the line integral (equation (1)), when $\boldsymbol{X}$ approaches $\boldsymbol{R}$. A standard cut-off technique is used to de-singularize the BS integral. The integral is split into two parts: a local term, which represents the integral between two neighbouring mesh points at the singularity location and gives an induced velocity $\boldsymbol{u}_0$; and a non-local term, which represents the regular part of the integral and gives an induced velocity $\boldsymbol{u}_1$, so that

https://doi.org/10.1017/S0022112099005224 Published online by Cambridge University Press

$\boldsymbol{u} = \boldsymbol{u}_0 + \boldsymbol{u}_1$. Following Schwarz (1985), the local term is given by

$$\boldsymbol{u}_0 = \frac{\Gamma}{4\pi}(\boldsymbol{R}' \times \boldsymbol{R}'') \ln \frac{2(l_+ l_-)^{1/2}}{C r_{\text{core}}}, \tag{5}$$

where l_+ and l_- are the distances to the nearest neighbouring point. This choice for the local term gives the correct velocity for the osculating vortex ring. The constant C is determined by the choice of the core model: it is of order 1 and can be absorbed into the definition of the effective filament core size r_{core}, which is not an important parameter in these simulations. We normally run the code with a very small core parameter ($r_{\text{core}} = 10^{-8}$), and we have done tests where the core parameter was increased up to $r_{\text{core}} = 10^{-4}$. While the velocity changed in these tests, as it should, the qualitative behaviour of the knot evolution and the shape of the knot did not change.

To measure the changes in the knot shape and the degree of stability we introduce the concept of geometric growth of the radius of the torus circular axis in the (X, Y)-plane ('XY-growth') with time. The geometric growth is measured by $\Delta\epsilon = \epsilon - \epsilon_0$, where

$$\epsilon = \frac{R_{XY\max} - R_{XY\min}}{2}, \tag{6}$$

$R_{XY\max}(R_{XY\min})$ denoting the maximal (minimal) distance of the knot from its centre of symmetry (placed at the origin $r = 0$) in the (X, Y)-plane. Measurements of geometric growth will give us precise information about the geometric coherence of these vortex structures.

3.1. *Evolution under the localized induction approximation (LIA) law*

The evolution of vortex knots under the LIA equation is illustrated in the time sequence of figure 2. We find that vortex structures evolving under LIA behave in a way which is consistent with the stability criterion given by Theorem 3. For winding number $w > 1$, the knot is steady and stable, travelling along the z-axis for about 20 diameters (corresponding to about 23 time units) until numerical noise de-stabilizes the structure. For winding number $w < 1$, instability sets in almost immediately, leading to the unfolding of the vortex knot (see the time sequence of figure 3). The knot travels along the z-axis for not more than two diameters (notice the values of the z-coordinate), while unfolding irreversibly until the occurrence of the first knot self-intersection: at this point LIA becomes ill-defined and the calculation must be stopped. This evolution takes place in the first few time units.

The XY-growth is shown in figures 4(a) and 4(b). The instability seems to grow with a very clean power law, with power close to 2, until numerical errors become dominant. It is interesting to notice that we have similar results for the evolution of the unknots. For example we find that $\mathscr{U}_{1,3}$ retains its shape for a considerable time, whereas the corresponding toroidal counterpart $\mathscr{U}_{3,1}$ ($w = \frac{1}{3}$) unfolds immediately, following the same power law as for the other knot types tested. A summary of these results is given in figure 4(a), where the characteristics of the dynamics investigated are shown to be generic and independent of the specific knot type tested.

For larger values of $\epsilon_0 (\geqslant 0.1)$, the theory based on LIA is no longer applicable. However, the numerical analysis carried out has shown that these structures are much more robust and stable than previously thought. This means that an extended LIA theory (based on higher-order asymptotics) should be able to capture even 'large-amplitude' knot configurations as new steady and stable initial conditions for vortex motion.

https://doi.org/10.1017/S0022112099005224 Published online by Cambridge University Press

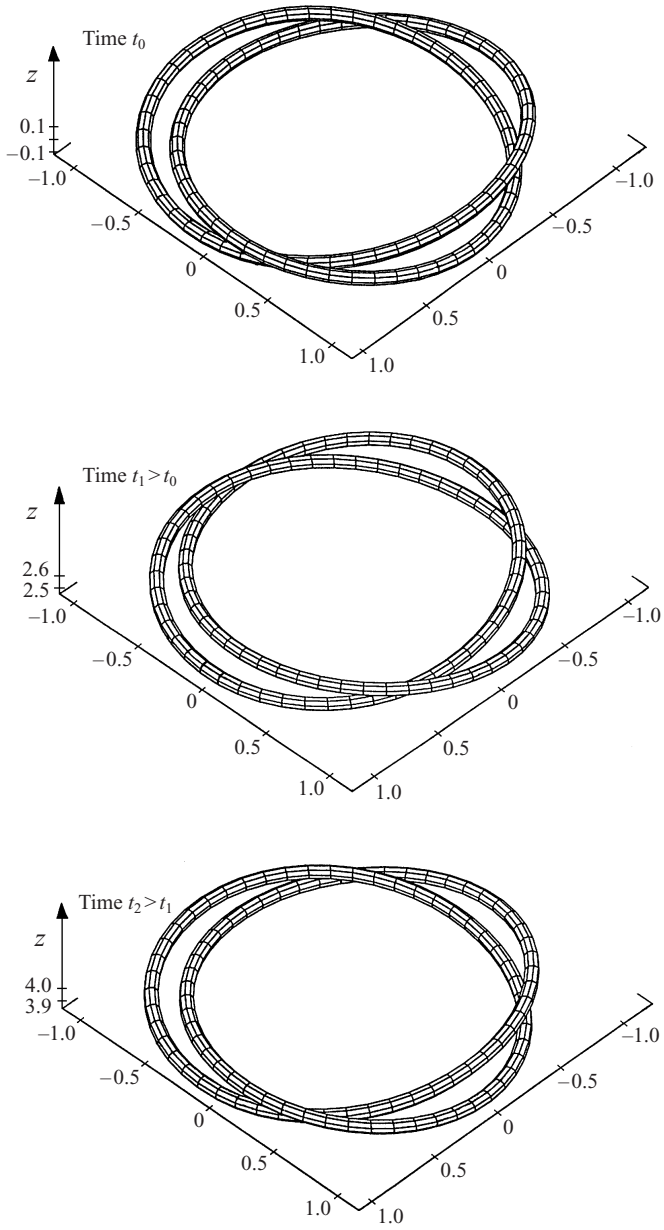


FIGURE 2. Computed evolution of $\mathscr{T}_{2,3}$ under the LIA. The knot moves while maintaining its shape in a stable manner, which is consistent with Theorem 3. Snapshots of the vortex knot evolution are shown at three different times $t_0 > t_1 > t_2$. Note the different values of the z-coordinate. In order to visualize over- and under-crossings a mathematical tube of radius 0.04 is centred on the knot axis. This tube is merely a visual aid, whose geometry has nothing to do with the real core cut-off size.

3.2. *Evolution under the Biot–Savart (BS) law*

When a given knot evolves under the full BS law we observe a very different behaviour. Figures 5(*a*) and 5(*b*) show a comparison of $\mathscr{T}_{2,3}$ ($w = \frac{3}{2}$) and $\mathscr{T}_{3,2}$ ($w = \frac{2}{3}$) under LIA and BS evolution, for $\epsilon_0 = 0.01$ and 0.1 (LIA), and $\epsilon_0 = 0.1$ (BS). Remarkably, we find that both the knot $\mathscr{T}_{2,3}$ and its isotope $\mathscr{T}_{3,2}$ (with winding number $w < 1$) maintain

https://doi.org/10.1017/S0022112099005224 Published online by Cambridge University Press

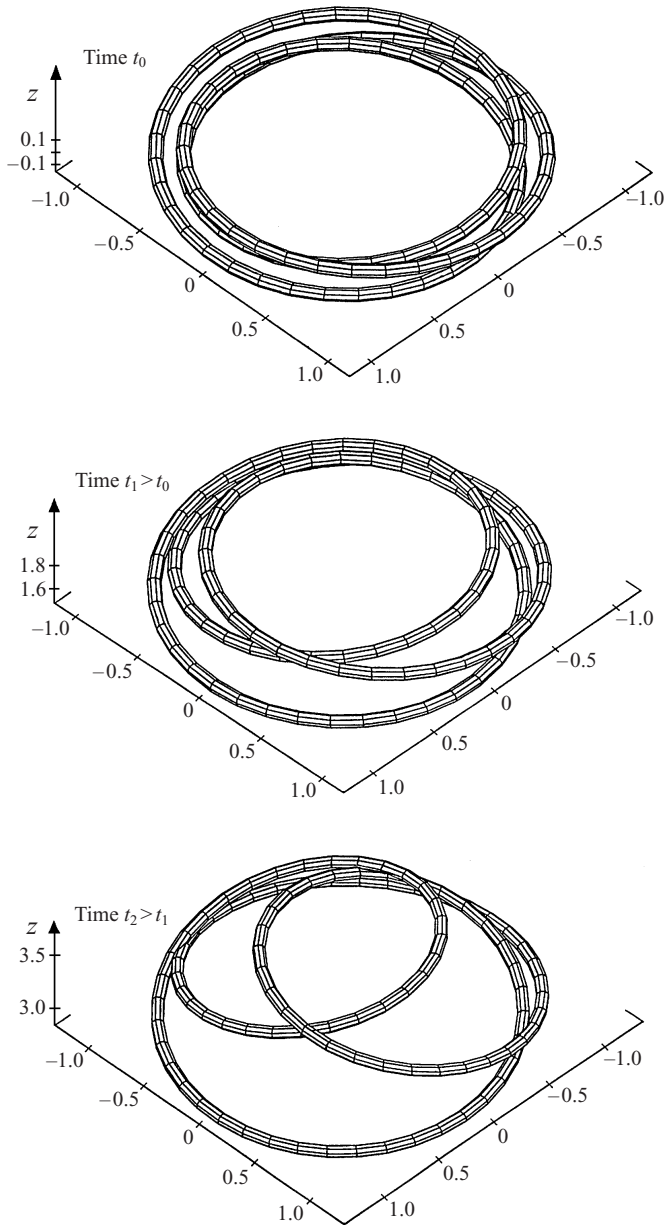


FIGURE 3. Computed evolution of $\mathcal{T}_{3,2}$ under LIA. The knot unfolds, which is consistent with Theorem 3. The last picture of the time sequence (at time t_2) shows the unfolding knot approaching a self-intersection (same visualization as for figure 2).

their shape under the BS law for a long time, travelling without unfolding for about 20 diameters, until numerical noise sets in. The visible 'wiggling' in the plots (which is particularly enhanced in the case of the BS law) is a signature of the oscillatory geometry of the knot. This behaviour appears to be independent of filament core size and discretization parameters (we have run the code for different N) and we did not find any significant difference for the other knot types tested.

Vortex torus knots evolving under the BS law are clearly 'stabilized' by global

https://doi.org/10.1017/S0022112099005224 Published online by Cambridge University Press

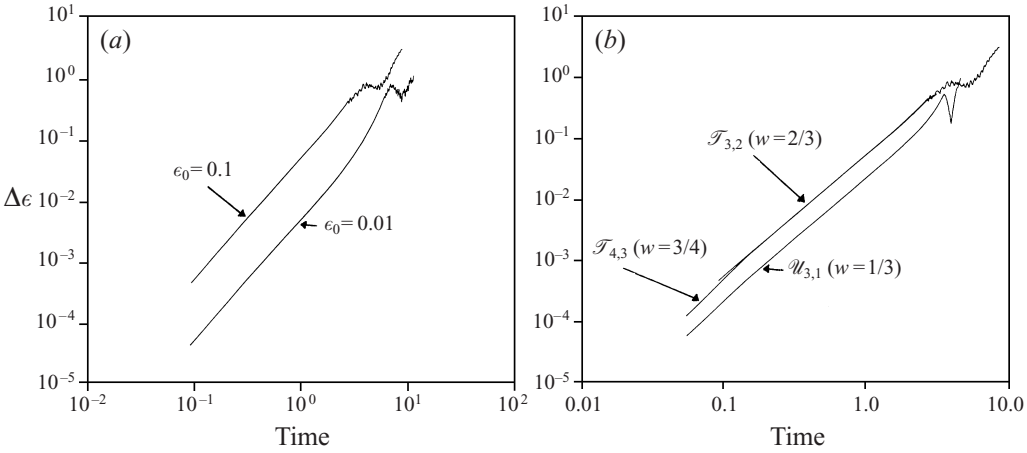


FIGURE 4. LIA evolution. The dynamical instability of vortex knots is measured by the 'XY-growth' given by the variation of $\Delta\epsilon$ with time. Vortex structures are found to be LIA-stable when their winding number is $w > 1$ and LIA-unstable when $w < 1$, which is consistent with the prediction of Theorem 3. (*a*) The growth in ϵ_0 for the torus knot $\mathscr{T}_{3,2}$ ($w = 2/3$) with initial $\epsilon_0 = 0.1$ and $\epsilon_0 = 0.01$. (*b*) The growth in ϵ_0 for the knots $\mathscr{T}_{3,2}$ ($w = 2/3$) and $\mathscr{T}_{4,3}$ ($w = 3/4$), and for the (unknotted) toroidal coil $\mathscr{U}_{3,1}$ with initial $\epsilon_0 = 0.1$.

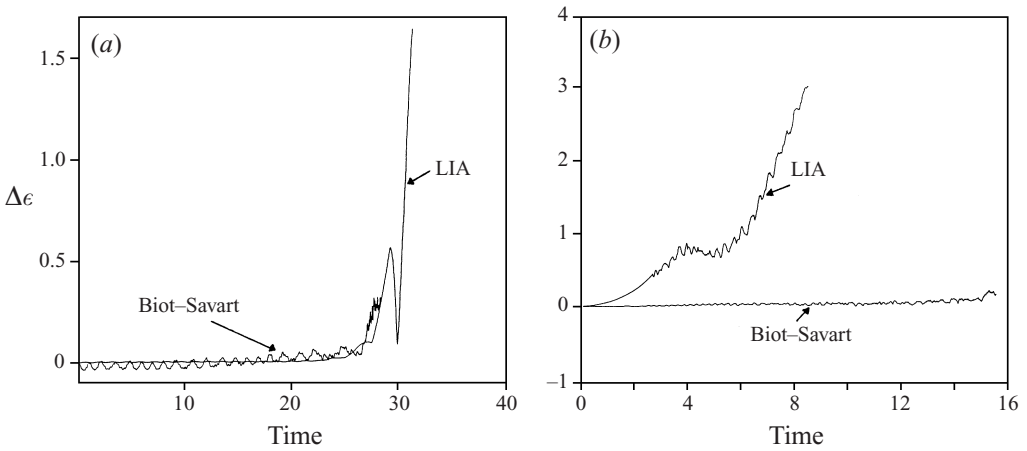


FIGURE 5. BS evolution. Comparative behaviour of (*a*) $\mathscr{T}_{2,3}$ and (*b*) $\mathscr{T}_{3,2}$ ($\epsilon_0 = 0.1$) under the LIA and BS law: the knot $\mathscr{T}_{2,3}$ ($w = \frac{3}{2}$) travels under both the LIA and BS law without change of shape for about 20 diameters, until the numerical noise sets in. The knot $\mathscr{T}_{3,2}$ ($w = \frac{2}{3}$) unfolds under LIA (as predicted by Ricca 1995), but is stabilized when its evolution is governed by the BS law. Under LIA the unfolding takes place almost immediately.

geometric effects. This stabilizing effect is due to the BS integration (figure 5*b*) and is the main result of these calculations. A three-dimensional view of the BS knot evolution is given by the time sequence of figure 6. The motion is the sum of two contributions: one is due to a propagation velocity that makes the whole structure translate in the fluid; the other is due to a rotational velocity that makes the individual vortex strands rotate around their centre of mass (which lies in the meridian plane on the torus circular axis) and around each other. This second contribution is difficult to

https://doi.org/10.1017/S0022112099005224 Published online by Cambridge University Press

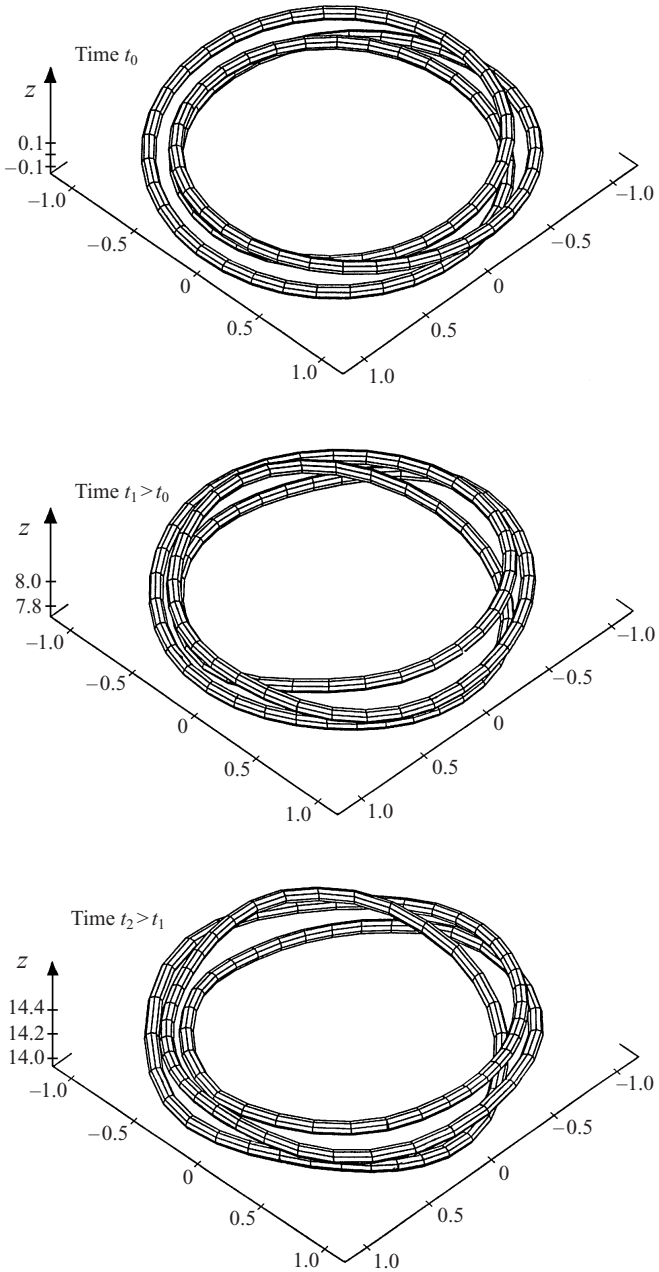


FIGURE 6. BS evolution of $\mathscr{T}_{3,2}$. The knot evolution is rather stable and the vortex travels a large distance (see z-values at time t_2) before the numerical noise sets in (same visualization as for figure 2).

detect from the plots of figure 6, but it is very clear from the moving pictures of the vortex evolution.

Does the stabilizing effect of the BS law depend on ϵ_0? Figure 7 shows the evolution of $\mathscr{T}_{3,2}$ for different values of ϵ_0, under both the BS law and LIA (for comparison). In this case geometric coherence is measured by the time $T_{\rm rec}$ elapsed at the occurrence

https://doi.org/10.1017/S0022112099005224 Published online by Cambridge University Press

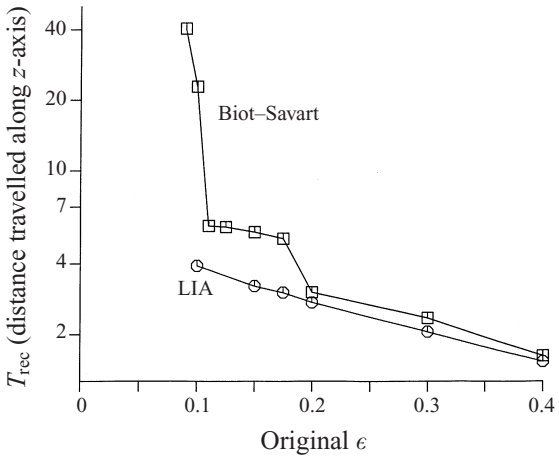


FIGURE 7. The time $T_{\rm rec}$ elapsed until the occurrence of the first self-intersection (proportional to the distance travelled by the knot along the z-axis) against the original ϵ for the LIA (circles) and BS (squares) evolution. Note that the plot is on a logarithmic scale.

of the first self-intersection, which leads to the following re-structuring and unfolding of the vortex knot. For $\epsilon_0 > 0.2$ geometric coherence is definitely lost and the BS law is no longer able to guarantee stable evolution. Under LIA the power law dependence of $T_{\rm rec}$ (the straight line on the log-scale diagram) indicates that ϵ_0 is in fact the parameter that controls the stability of the structure (in agreement with Ricca 1995), whereas under the BS law we find a critical threshold value at $\epsilon_{0\rm crit} \approx 0.1$, above which stability is lost. When ϵ_0 is small, vortex line elements are so close to each other that a large number N of discretization points is needed. In principle the BS integration is an N^2 operation, because the motion of each point is determined by the position of all the others, but in practice the computer time required for the calculation increases even faster than N^2 (this is because the time step decreases in proportion to the mesh size, so that the distance travelled during one time step remains significantly less than the mesh size).

What is the reason for the BS stabilization? A possible explanation may be found in the cooperative swirling motion of the co-rotating vortex strands (see Saffman 1992, § 12.2). In the first stages of the evolution the individual vortex strands are very close and nearly parallel to one another. Under the BS law these elements rotate about one another, orbiting about their centre of mass (in the meridian plane), a motion that is completely missed by the LIA. This motion makes the vortex structure rotate on itself, as if the whole structure were subject to a virtual twist. This corresponds of course to the familiar rotation of smoke rings. From figure 3, which illustrates the LIA unfolding of the unstable knot, one can see that this process is due to the faster motion of the high-curvature elements of the vortex filament in the interior region of the knot, relative to the slower motion of the low-curvature elements in the outer region. Under the LIA we have no rotation of the individual strands and the motion is simply a translation in the binormal direction. When the knot translates and rotates on itself, though, these inner and outer parts of the knot exchange places during rotation. If their rotation is fast enough, it can average out the translational velocity of the vortex, leading to a more uniform motion of the filament and a stabilization of the vortex knot (a mechanism that resembles the co-rotating vortex pair stability to long-wave disturbances investigated by Jiménez 1975).

https://doi.org/10.1017/S0022112099005224 Published online by Cambridge University Press

An estimate of this rotational velocity ($V_{\rm rot}$) is given by considering the rotational velocity of p straight vortex lines equally spaced on a circle of radius ϵ_0. This gives

$$V_{\rm rot} \simeq p\Gamma/4\pi\epsilon_0. \tag{7}$$

An estimate of the translational velocity ($V_{\rm trans}$) of a vortex ring of radius r_0 gives

$$V_{\rm trans} \simeq \frac{\Gamma}{4\pi r_0} \ln \frac{8r_0}{r_{\rm core}}. \tag{8}$$

The ratio of the two velocities is

$$\frac{V_{\rm rot}}{V_{\rm trans}} = \frac{r_0 p}{\epsilon_0 \ln (8r_0/r_{\rm core})}. \tag{9}$$

For $p = 3$ and $r_{\rm core} = 10^{-8}$ we have $V_{\rm rot}/V_{\rm trans} > 1$ when $\epsilon < 0.15r_0$ (i.e. rotation dominates), and this is remarkably close to the data shown in figure 7.

The fact that the BS evolution may differ significantly from the LIA evolution provides a clear demonstration that the LIA law is not appropriate to investigate the long-term behaviour of complex flow dynamics. From a computational viewpoint the identification of flows which require the BS law also has important practical consequences in the implementation of effective numerical codes.

4. Conclusions

We have performed numerical investigations of the evolution of vortex knots under both the LIA and the BS law. When the parameters are close to the vortex knots of Ricca's theory, we find that vortex knots either translate while maintaining their shape, or unfold immediately, in a way which is consistent with Ricca's stability theory. We have also observed that the way in which the knots unfold (see figure 4) appears to be independent of the topology: all unstable torus knots and unknots show the same power law growth in amplitude.

The most important result is the discovery of a strong stabilizing effect of the BS law. Although we find that knots eventually unfold, the time which elapses and the distance over which they travel before breaking up is very large and has physical significance. This finding suggests that it is worth trying to create vortex knots in the laboratory. For relatively large values of ϵ_0 we have found cases (see figure 4) in which the BS evolution is almost identical to the evolution under LIA. These results will certainly stimulate more numerical work and, above all, the search for a new analytical theory for the existence of steady and stable vortex knot solutions to the Euler equations.

From a physical viewpoint, then, these results shed new light on the evolution of complex structures, and are useful for future modelling of turbulent flows. Our measures of the geometric coherence of vortex knot dynamics clearly show that there are complex flow fields resistant to re-structuring, which is a very important feature in relation to the role and decay of helicity in turbulent flows (Moffatt & Tsinober 1990).

Finally, we would like to point out another result that comes out from these numerical simulations: torus knots with winding number $w < 1$ are in general unstable and evolve under the BS law towards a reconnection event (although in the case of thin filaments this might take place on much longer time scales). This result is significant in view of the great interest in the formation of singularities in Euler's equations (Kerr 1993; Fernandez *et al.* 1995; Grauer & Sideris 1995; Greene

https://doi.org/10.1017/S0022112099005224 Published online by Cambridge University Press

& Boratav 1997). Our work shows that vortex knots are a simple and effective means for investigating mechanisms of singularity formation in ideal fluids and other related questions.

R.L.R. would like to acknowledge financial support from The Leverhulme Trust. C.F.B.'s research is funded by an equipment grant from The Royal Society of London.

REFERENCES

Aarts, R. G. K. & deWaele, A. T. A. M. 1994 Numerical investigation of the flow properties of He II. *Phys. Rev.* B **50**, 1069–1079.

Barenghi, C. F. 1997 Vortex lines and transitions in superfluid hydrodynamics. *Phil. Trans. R. Soc. Lond.* A **355**, 2025–2034.

Barenghi, C. F., Samuels, D. C., Bauer, G. H. & Donnelly, R. J. 1998 Vortex lines in a model of turbulent flow. *Phys. Fluids* **9**, 2631–2643.

Batchelor, G. K. 1967 *An Introduction to Fluid Dynamics*. Cambridge University Press.

Berger, J. & Rubinstein, J. 1997 Formation of topological defects in thin super-conducting rings. *Phil. Trans. R. Soc. Lond.* A **355**, 1969–1978.

Berger, M. A. 1993 Energy-crossing number relations for braided magnetic fields. *Phys. Rev. Lett.* **70**, 705–708.

Berger, M. A. & Field, G. B. 1984 The topological properties of magnetic helicity. *J. Fluid Mech.* **147**, 133–148.

Birman J. S. & Williams R. F. 1983 Knotted periodic orbits in dynamical systems I: Lorenz's equations. *Topology* **22**, 47–82.

Bray, R. J., Cram, L. E., Durrant, C. J. & Loughhead, R. E. 1991 *Plasma Loops in the Solar Corona*. Cambridge University Press.

Donnelly, R. J. 1991 *Quantized Vortex Lines in Helium II*. Cambridge University Press.

Fernandez, V. M., Zabusky, N. J. & Gryanik, V. M. 1995 Vortex intensification and collapse of the Lissajous-elliptic ring: single- and multi-filament Biot–Savart simulations and visiometrics. *J. Fluid Mech.* **299**, 289–331.

Grauer, R. & Sideris, T. C. 1995 Finite-time singularities in ideal fluids with swirl. *Physica* D **88**, 116–132.

Greene, J. M. & Boratav, O. N. 1997 Evidence for the development of singularities in Euler flows. *Physica* D **107**, 57–68.

Holmes P. J. & Williams R. F. 1985 Knotted periodic orbits in suspensions of Smale's horseshoe: torus knots and bifurcation sequences. *Arch. Rat. Mech. Anal.* **90**, 115–194.

Jiménez, J. 1975 Stability of a pair of co-rotating vortices. *Phys. Fluids* **18**, 1580–1581.

Jiménez, J., Wray, A. A., Saffman, P. G. & Rogallo, R. S. 1993 The structure of intense vorticity in homogeneous isotropic turbulence. *J. Fluid Mech.* **255**, 65–90.

Kelvin, Lord 1875 Vortex Statics. *Proc. R. Soc. Edinb.* Session 1875–76.

Kerr, R. M. 1985 Higher order derivative correlations and the alignment of small scale structures in isotropic numerical turbulence. *J. Fluid Mech.* **153**, 31–58.

Kerr, R. M. 1993 Evidence for a singularity of the three-dimensional, incompressible Euler equations. *Phys. Fluids* A **5**, 1725–1746.

Kida, S. 1981 A vortex filament moving without change of form. *J. Fluid Mech.* **112**, 397–409.

Koplick, J. & Levine, H. 1993 Vortex reconnection in superfluid helium. *Phys. Rev. Lett.* **71**, 1375–1378.

Leonard, A. 1980 Vortex methods for flow simulations. *J. Comput. Phys.* **37**, 239–335.

Leonard, A. 1985 Computing three-dimensional incompressible flows with vortex elements. *Ann. Rev. Fluid Mech.* **17**, 523–559.

Leonard, A. & Chua, K. 1989 Three-dimensional interactions of vortex tubes. *Physica* D **37**, 490–496.

Lugomer, S. 1998 Observation of solitons on vortex-filament bush. *Phys. Lett.* A **242**, 319–325.

Lugt, H. J. 1983 *Vortex Flow in Nature and Technology*. Wiley.

Massey, W. S. 1967 *Algebraic Topology: An Introduction*. Harcourt, Brace and World, New York.

https://doi.org/10.1017/S0022112099005224 Published online by Cambridge University Press

Moffatt, H. K. 1969 The degree of knottedness of tangled vortex lines. *J. Fluid Mech.* **36**, 117–129.

Moffatt, H. K. & Ricca, R. L. 1992 Helicity and the Călugăreanu invariant. *Proc. R. Soc. Lond.* A **439**, 411–429.

Moffatt, H. K. & Tsinober, A. (Eds.) 1990 *Topological Fluid Mechanics*. Cambridge University Press.

Moffatt, H. K., Zaslavsky, G. M., Comte, P. & Tabor, M. (Eds.) 1992 *Topological Aspects of the Dynamics of Fluids and Plasmas*. Kluwer.

Moin, P., Leonard, A. & Kim, J. 1986 Evolution of a curved vortex filament into a vortex ring. *Phys. Fluids* **29**, 955–963.

Ricca, R. L. 1993 Torus knots and polynomial invariants for a class of soliton equations. *Chaos* **3**, 83–91 (and Erratum. *Chaos* **5**, 1995, 346).

Ricca, R. L. 1995 Geometric and topological aspects of vortex filament dynamics under LIA. In *small-Scale Structures in Three-Dimensional Hydro and Magnetohydro-dynamics Turbulence* (ed. M. Meneguzzi *et al.*), pp. 99–104. Lecture notes in Physics, vol. 462. Springer.

Ricca, R. L. 1996 The contributions of Da Rios and Levi-Civita to asymptotic potential theory and vortex filament dynamics. *Fluid Dyn. Res.* **18**, 245–268.

Ricca, R. L. 1998 Applications of knot theory in fluid mechanics. In *Knot Theory* (ed. V. F. R. Jones *et al.*), vol. 42, pp. 321–346. Banach Center Publications, Institute of Mathematics, Polish Academy of Sciences, Warszawa.

Ricca, R. L. & Berger, M. A. 1996 Topological ideas and fluid mechanics. *Phys. Today* **49** (12), 24–30.

Saffman, P. G. 1992 *Vortex Dynamics*. Cambridge University Press.

Samuels, D. C. 1992 Velocity matching and Poiseuille pipe flow of superfluid helium. *Phys. Rev.* B **46**, 11714–11724.

Samuels, D. C. 1998 A finite length instability of vortex tubes. *Eur. J. Mech.* B/*Fluids* **17**, 587–594.

Samuels, D., Barenghi, C. & Ricca, R. L. 1998 Quantized vortex knots. *J. Low Temp. Phys.* **110**, 509–513.

Schwarz, K. W. 1985 Three-dimensional vortex dynamics in superfluid He 4: line-line and line-boundary interactions. *Phys. Rev.* B **31**, 5782–5804.

Schwarz, K. W. 1988 Three-dimensional vortex dynamics in superfluid helium. *Phys. Rev.* B **38**, 2398–2417.

She, Z.-S., Jackson, E. & Orszag, S. A. 1990 Intermittent vortex structures in homogeneous isotropic turbulence. *Nature* **344**, 226–228.

Vincent, A. & Meneguzzi, M. 1991 The spatial structure and statistical properties of homogeneous turbulence. *J. Fluid Mech.* **225**, 1–25.

Zabusky, N. J., Silver, D. & Pelz, R. 1993 Visiometrics, juxtaposition and modelling. *Phys. Today* **46**, 24–31.

Zhou, H. 1997 On the motion of slender vortex filaments. *Phys. Fluids* **9**, 970–981.

https://doi.org/10.1017/S0022112099005224 Published online by Cambridge University Press